Published in final edited form as:
Biochemistry. 2009 July 28; 48(29): 6772–6782. doi:10.1021/bi900472a.

Bases in 16S rRNA Important for Subunit Association, tRNA binding, and Translocation

Xinying Shi, **Katie Chiu**, **Srikanta Ghosh**, and **Simpson Joseph***
Department of Chemistry and Biochemistry, University of California, San Diego, 9500 Gilman Drive, La Jolla, CA 92093-0314.

Abstract

Ribosomes are the cellular machinery responsible for protein synthesis. A well-orchestrated step in the elongation cycle of protein synthesis is the precise translocation of the tRNA-mRNA complex within the ribosome. Here we report the application of a new *in vitro* modification-interference method for the identification of bases in 16S rRNA that are essential for translocation. Our results suggest that conserved bases U56, U723, A1306, A1319, and A1468 in 16S rRNA are important for translocation. These five bases were deleted or mutated in order to study their role in translation. Depending on the type of mutation, we observed inhibition of growth rate, subunit association, tRNA binding and/or translocation. Interestingly, deletion of U56 or A1319 or mutation of A1319 to C showed a lethal phenotype and were defective in protein synthesis *in vitro*. Further analysis showed that deletion of U56 or A1319 caused defects in 30S subunit assembly, subunit association and tRNA binding. In contrast, A1319C mutation showed no defects in subunit association; however, the extent of tRNA binding and translocation was significantly reduced. These results show that conserved bases located as far away as 100 Å from the tRNA binding sites can be important for translation.

Keywords

ribosome; mRNA; tRNA; translocation; EF-G, 16S rRNA

Ribosomes contain three tRNA binding sites: the aminoacyl site (A site), the peptidyl site (P site), and the exit site (E site). During protein synthesis, A and P site tRNAs move in a precise and coordinated manner to the P and E sites, respectively. Early biochemical and biophysical studies showed that the movement of the tRNAs occurs in two steps (1,2). First, following peptide bond formation, the acceptor ends of deacylated and peptidyl tRNAs translocate spontaneously into the 50S subunit's E and P sites, respectively. The anticodon ends of deacylated and peptidyl tRNAs maintain their interactions with the 30S subunit's P and A sites, respectively, resulting in hybrid P/E and A/P binding states. Second, EF-G binds to the ribosome and hydrolyzes GTP. GTP hydrolysis accelerates the translocation of the anticodon end of the tRNAs and the associated mRNA by one codon relative to the 30S subunit (3). Recent experiments are consistent with a step wise movement of the tRNAs through the ribosome (4-10).

*Correspondence to: Simpson Joseph 4102 Urey Hall, Department of Chemistry and Biochemistry, University of California, San Diego, 9500 Gilman Drive, La Jolla, CA 92093-0314. Phone: (858) 822-2957 Fax: (858) 534-7042 sjoseph@chem.ucsd.edu.

SUPPORTING INFORMATION AVAILABLE

Data showing site-specific cross-linking of *E. coli* $tRNA_1^{Val}$ to 16S rRNA, translocation of 3'-biotin-$tRNA_1^{Val}$ from the A site, analysis of ribosomal proteins present in mutant subunits by two-dimensional gel electrophoresis, *in vitro* protein synthesis by mutant ribosomes, structural changes in 16S rRNA of the mutant ribosomes, and primer extension analysis of 30S subunits purified using the MS2 affinity tag. This material is available free of charge via the Internet at http://pubs.acs.org

Strikingly, during translocation, the ribosome goes through large-scale conformational changes as shown by cryo-EM reconstruction of stalled translocation intermediates (11-14). The changes depicted by cryo-EM showed the large and small ribosomal subunits undergoing a ratchet like movement relative to each other during translocation. This indicates that translocation involves multiple conformational changes in both subunits. However, conformational changes in the ribosome are not well understood and the molecular basis of translocation is not yet clear.

Numerous studies suggest that the rRNAs play an important role during translocation. First, mutations or modifications in rRNAs confer resistance to antibiotics, such as viomycin, thiostrepton, and spectinomycin, that block specific steps in translocation (15-17). Most of these antibiotics protect nucleotides in rRNAs from chemical probes indicating that they bind directly to the rRNAs (18,19). Indeed, this has been confirmed by recent x-ray crystallographic studies, which showed that antibiotics that inhibit translocation, such as thiostrepton, spectinomycin and hygromycin B, mainly contact the rRNAs (20-23). Second, EF-G protects nucleotides in 23S rRNA and has been cross-linked to 23S rRNA suggesting that contacts with the rRNAs are critical for translocation (24,25). Third, disruption of specific interactions between the tRNAs and the rRNAs inhibit translocation (7,26-29).

Even though high-resolution structures of the ribosome are now available, it is difficult to predict which bases in the rRNAs are important for specific steps in translation. This gap in understanding the functional significance of the structure needs to be filled by biochemical and biophysical studies that analyze interesting features revealed by the structures. However, systematically interrogating individual bases for their functional role in translation can become tedious and expensive. On the other hand, modification-interference methods allow the simultaneous analysis of many residues in one experiment, and have been used for identifying functionally important nucleotides in a variety of RNA structures, RNA-protein complexes and catalytic RNAs. Specifically, modification-interference methods have proven useful for identifying bases in rRNA that are essential for tRNA binding to the ribosomal A and P sites (30-32). Here, we describe a powerful *in vitro* modification-interference method for identifying bases in 16S rRNA that are critical for translocation. The modification-interference method is based on the site-specific cross-linking of tRNA to 16S rRNA in ribosomes that have undergone translocation. Using this modification-interference approach, eleven bases were identified that may play an important role during translocation. Interestingly, five of these bases have never been implicated as being important for translation. These five bases were mutated in the 16S rRNA and the 16S rRNA mutants were systematically analyzed to examine their role in translation. Our results show that these bases located remotely from the tRNA binding sites affect subunit association, tRNA binding to the P site, and translocation of mRNA-tRNA complex by the ribosome.

Experimental Procedures

DNA cloning and transcription of gene32val2mRNA

A plasmid (pG32mRNA) encoding the T7 RNA polymerase promoter and a fragment of phage T4 gene 32 mRNA from position –55 to +85 was used for constructing a mutant mRNA with a valine codon at the second position. This was accomplished by replacing the Pac I-Pme I fragment with an appropriate double-stranded deoxyoligonucleotide containing a T to G transversion at the +4 position. The clone (pG32VAL2) with a valine codon (GUU) at the second position was identified by restriction digest analysis and sequencing. Plasmid pG32VAL2 was linearized with Bam HI and used as a template for *in vitro* transcription using T7 RNA polymerase to generate gene32val2 mRNA.

Construction of defined pre-translocation complex

Biotin was attached to the 3' end of deacylated *E. coli* $tRNA^{Val}_1$ (Subriden) as previously described (30). Pre-translocation complexes were formed by activating 50 pmol of tight-couple 70S at 42 °C for 10 min in binding buffer [80 mM potassium cacodylate (pH 7.2), 20 mM magnesium acetate, 150 mM ammonium chloride] followed by incubation at 37 °C for 10 min. 150 pmol of gene32val2 mRNA was added to the ribosomes and the complexes were incubated at 37 °C for 6 min. Next, 100 pmol of deacylated *E. coli* $tRNA_f^{Met}$ (Sigma) was added and the complexes were incubated at 37 °C for 30 min followed by addition of 100 pmol of 3'-biotin-$tRNA^{Val}_1$ and incubation at 37 °C for 30 min. Pre-translocation complexes (100 μl final volume) were placed on ice for 10 min. Pre-translocation complexes were modified by the addition of either 6 μl kethoxal (37 mg/ml) or 6 μl DMS (1:10 dilution in 95% ethanol) or 100 μl CMCT (42 mg/ml in binding buffer) for 10 min at 37 °C. For CMCT modification, the complexes were formed in 75 mM potassium borate (pH 7.0), 20 mM magnesium acetate, and 150 mM ammonium chloride. Reagents were removed by centrifugation in microcon 30 filtration units (Amicon) at 4 °C and concentrated to 48 μl final volume. In some of the experiments shown in Figure 1, $tRNA^{Val}_1$ or 3'-biotin-$tRNA^{Val}_1$ were bound directly to the ribosomal P site by omitting $tRNA_f^{Met}$ during complex formation.

Selection of 16S rRNAs from post-translocation complexes

Translocation was initiated by the addition of 50 pmol (1 μM) EF-G and 120 μM GTP (final concentration) to 48 μl of the modified pre-translocation complexes and incubating at 37 °C for 5 min. The reaction mixtures were transferred to a 96-well plate that was placed on crushed ice and irradiated with ultraviolet light of 312 nm wavelength (8000 $\mu w/cm^2$ intensity) for 10 min. Preliminary experiments indicated that this was sufficient to generate enough cross-linked material for streptavidin capture and primer extension analysis without damaging the ribosomes. The samples were extracted four times with water-saturated phenol followed by three chloroform extractions and the rRNAs were recovered by ethanol precipitation (33). The rRNAs were resuspended in 250 μl water (total rRNA population). 16S rRNAs, cross-linked to 3'-biotin-$tRNA^{Val}_1$, were captured using magnetic streptavidin beads (streptavidin-M280; Dynal). The beads were pre-washed to remove ribonucleases as recommended by the manufacturer. Next, 125 μl of the total rRNA mixture was gently mixed with 100 μl of streptavidin beads and the samples were processed using the manufacturer's supplied instruction. The beads were resuspended in 60 μl of water (selected 16S rRNA population). The level of modification within the 16S rRNAs from the total and the selected populations were examined by primer extension analysis as previously described (33). All experiments were repeated independently at least three times and the modification levels were quantified using a Phosphorimager (Molecular Dynamics). The values were normalized for sample loading differences and the background level estimated from the unmodified control lane was subtracted.

Toeprinting assay

Pre-translocation complexes were formed as described above and translocation was monitored by the toeprinting assay as described previously (34).

Site-directed mutagenesis of 16S rRNA

Site-directed mutagenesis was performed with a Quick Change PCR mutagenesis kit (Stratagene). Plasmid pKK3535 was used as a template for introducing mutations U56A, U723A, A1306U, A1319C and A1468U in 16S rRNA. All the remaining mutations and deletions were made using plasmid pLK35-16S-MS2 to facilitate purification of lethal mutants using the MS2 affinity tag method (29,35). All clones were verified by automated DNA sequencing of the entire 16S rRNA operon.

Plasmid-replacement strategy

Plasmid replacement was performed as described (36,37). Briefly, *E. coli* strain SQZ10 (Δ7rrn) containing plasmid pHK-rrnC^{+}sacB (kanamycin resistant) was transformed with pKK3535 or pLK35-16S-MS2 containing the desired mutations. The transformants were grown over night in LB media (10 g tryptone, 5 g yeast extract, 10 g NaCl per liter of media) with 100 μg/ml ampicillin at 37 °C with shaking. The cultures were diluted and plated on 2YT agar plates with 8% sucrose and 100 μg/ml ampicillin. The colonies on the plates were screened for sensitivity to kanamycin by replica plating. Plasmid replacement was confirmed by isolating plasmids and automated DNA sequencing. Cell stocks were prepared in 15% glycerol and stored at −80 °C.

Growth curve

Growth of plasmid-replaced *E. coli* strain SQZ10 (Δ7rrn) expressing wild-type or mutant 16S rRNA were carried out in 200 μl LB media in the presence of 100 μg/ml ampicillin at 37 °C with continuous shaking in a plate reader (Genios, Tecan). Each culture was inoculated with the same number of cells from overnight starter cultures. The absorbance at 600 nm wavelength was automatically measured every 10 minutes by the plate reader. The data was fit to an exponential growth curve equation ($Y = Ae^{bx}$), and the doubling time was calculated as In(2)/b using Prism (GraphPad Prism, San Diego, CA).

Polysome profile

Polysome profiles of *E. coli* strain SQZ10 (Δ7rrn) expressing wild-type or mutant 16S rRNA were determined essentially as described previously (38). Briefly 100 ml of plasmid-replaced SQZ10 cells were grown at 37 °C in the presence of 100 μg/ml ampicillin until the absorbance at 600 nm wavelength was 0.5. Then, 400 μg of chloramphenicol (final conc.) was added to the cell culture and immediately placed on ice. Cells were harvested and resuspended in 500 μl of 20 mM Tris (pH 7.5) and 15 mM $MgCl_2$. The cells were then lysed with lysozyme (1 mg/ml final conc.) and two freeze-thaw cycles in dry-ice ethanol bath. Then 25 μl of 10% deoxycholate (sodium salt) was added and the cell extracts were incubated on ice for 20 minutes. The absorbance of the extracts were measured at 260 nm and 0.6 mg ribosome equivalent were loaded onto a 10-40% sucrose gradient containing 20 mM Tris, pH 7.5, 10 mM $MgCl_2$, 100 mM NH_4Cl and 2 mM β-mercaptoethanol. The samples were fractionated by ultracentrifugation at 35,000 rpm for 4 hours and the gradients were profiled at 254 nm using an UA6 detector (ISCO).

Purification of MS2-tagged 30S subunits and subunit association

Mutations U56Δ, A1319Δ or A1319C are lethal and were purified from pop 2136 cells using the MS2 affinity tag. Expression and purification were performed as described (39). The purity of the MS2-tagged preparations was assayed by primer extension after total RNA extraction. Reverse transcription using the primer 5'-CCCGTCCGCCACTCGTCAGC-3' and NTP(-dCTP) +ddCTP gave different products for tagged and untagged 16S rRNA.

Subunit association was carried out by incubating 1.5-fold excess of 50S subunits over 30S in polyamine buffer (20 mM Hepes-KOH pH 7.6, 6 mM $MgCl_2$, 150 mM NH_4Cl, 4 mM β-mercaptoethanol, 0.05 mM spermine and 2 mM spermidine).(40,41), but with 20 mM $MgCl_2$ for 10 min at 42 °C, slow cooling to 37 °C and another 15 min at 37 °C. The solution was diluted with the same buffer with no $MgCl_2$ to lower its concentration to 6 mM, and further incubated for 15 additional minutes at 37 °C. For analyzing subunit association by sucrose gradient centrifugation, we tested different concentrations of $MgCl_2$ ranging from 10 mM to 20 mM. The sucrose gradients were prepared in 50 mM Tris-HCl (pH 7.6), 100 mM NH_4Cl and 6 mM β-mercaptoethanol with 10 mM or 20 mM $MgCl_2$.

Two-dimensional gel electrophoresis

Ribosomal proteins from the 30S subunits were isolated by acetic acid extraction as described (42) and suspended in 10 μl loading buffer containing 8 M urea, 1% 2-mercaptoethanol and 10 mM Bis-tris acetate (pH 4.1), and analyzed by two-dimensional gel electrophoresis (43). The proteins were visualized by staining with 0.25% coomassie brilliant blue. The gels were scanned at 600 dpi and the proteins quantified using ImageOne software (Bio-Rad).

In vitro translation of reporter protein

The activity of the purified ribosomes was analyzed by *in vitro* translation of the reporter protein Renilla luciferase as described previously (29). Briefly, activated ribosomes were added to the S-100 *in vitro* translation mix and transferred to a 96-well plate. The 96-well plate was incubated at 37 °C in a plate reader (Genios, Tecan) and the synthesis of luciferase enzyme was monitored in real-time by measuring the luminescence every 2 minutes. Duplicates of the samples were performed for each experiment and the assays were repeated at least two times.

tRNA binding

We used the toeprinting assay for determining the binding of $tRNA^{fMet}$ to the P site (44). Briefly, activated 30S subunits (0.4 μM final conc.) in polyamine buffer was incubated for 10 min at 37 °C with gene 32 mRNA fragment (0.8 μM final conc.) having the AL2 primer annealed to the 3'-end. Then aliquots of the 30S-mRNA mix were added to tubes containing different amounts of $tRNA^{fMet}$ (0 to 4 μM final conc.) prepared in polyamine buffer. The tubes were incubated at 37 °C for 30 min to allow binding of $tRNA^{fMet}$ to the P site. The complexes were analyzed by extending the AL2 primer with reverse transcriptase and separating the products on denaturing polyacrylamide gels. The toeprints were quantified by phosphorimager, as previously described (34). The amount of tRNA bound = bound/(free + bound) (44).

We used filter binding as a second method to quantify the amount of $tRNA^{fMet}$ bound to the 30S subunits (28). Filter binding experiments were performed in 80 mM K-cacodylate (pH 7.2), 7 mM $MgCl_2$ and 150 mM NH_4Cl because the presence of polyamines increased the non-specific background counts.

Translocation kinetics

Rapid kinetic experiments were performed essentially as described previously (45). The experiments were done at 25 °C in polyamine buffer. Briefly, 80 μl of pre-translocation complex (0.25 μM, after mixing) containing $tRNA_f^{Met}$ and fMet-Phe-$tRNA^{Phe}$ in ribosomal P and A sites, respectively, and pyrene-labeled mRNA+9 was rapidly mixed with 80 μl of EF-G●GTP (1.25 μM, after mixing) using a stopped-flow instrument (μSFM-20, BioLogic, France). The samples were excited at 343 nm wavelength and the change in fluorescence emission intensity at 376 nm was measured after passing through a long-pass filter 361 AELP (Omega Optical, VT, USA). About 5 traces were averaged for each experiment and the experiments were repeated four times. The decrease in fluorescence intensity were analyzed by non-linear least-squares fitting to the double exponential equation $Y = a*x+b + A_1*\exp(-k_1*x) + A_2*\exp(-k_2*x)$ using Bio-Kine software (BioLogic, France).

Results

Modification-Interference Analysis

More than three decades ago Ofengand, Zimmerman, and co-workers identified a site-specific cross-link formed between nucleotide cmo^5U34 of P site bound $tRNA_1^{Val}$ and C1400 of 16S rRNA (46,47). This cross-link was formed in high yield (up to 70%) when the complex was irradiated with ultraviolet light of 300-400 nm wavelength (47). *E. coli* $tRNA_1^{Val}$ and

$tRNA_1^{Ser}$ formed the cross-link, while $tRNA_f^{Met}$, $tRNA^{Phe}$ and $tRNA_2^{Val}$ did not form the cross-link (47). We repeated some of these experiments before setting up our *in vitro* selection method (Supplementary Figure 1). Consistent with previous studies, $tRNA_1^{Val}$ formed the cross-link to nucleotide C1400 of 16S rRNA when bound to the ribosomal P site, while $tRNA_f^{Met}$ did not form this cross-link (47) (Supplementary Figure 1A). No cross-link was observed when $tRNA_1^{Val}$ was bound to the ribosomal A site (Supplementary Figure 1B). This is in agreement with a previous report that high salt concentration (150 mM ammonium chloride) represses cross-linking to the A site (47). To facilitate selection, biotin was attached to the 3'-terminus of *E. coli* $tRNA_1^{Val}$. Attachment of biotin to the 3'-terminus of $tRNA_1^{Val}$ does not strongly affect the formation of the cross-link (Supplementary Figure 1C). Furthermore, only 16S rRNAs cross-linked to 3'-biotin-$tRNA_1^{Val}$ were captured by the streptavidin beads, while 16S rRNAs cross-linked to $tRNA_1^{Val}$ without the 3'-biotin does not bind to the streptavidin beads (data not shown). Thus, 16S rRNAs cross-linked to 3'-biotin-$tRNA_1^{Val}$ bind to the streptavidin beads only through the biotin moiety. Finally, $tRNA_1^{Val}$ and 3'-biotin-$tRNA_1^{Val}$ both translocate efficiently from the ribosomal A site to the P site (Supplementary Figure 1D). These features of the cross-link make it suitable for the efficient isolation of 16S rRNA from ribosomes that have undergone translocation as described below.

Pre-translocation complexes were formed by programming *E. coli* ribosomes with a defined mRNA sequence and deacylated $tRNA_f^{Met}$ and 3'-biotin-$tRNA_1^{Val}$ in the P and A sites, respectively (Figure 1A). The complexes were treated with base specific reagents dimethyl sulfate (DMS), 1-cyclohexyl-3-(2-morpholinoethyl) carbodiimide (CMCT) or kethoxal that modify rRNAs within the ribosome (Figure 1B). Treated pre-translocation complexes were incubated with EF-G•GTP to catalyze translocation. Translocation resulted in the movement of $tRNA_f^{Met}$ and $tRNA_1^{Val}$ into the E and P sites, respectively (Figure 1C). However, a fraction of the ribosomes do not undergo translocation due to the modification of bases in 16S rRNA that are important for translocation. In order to identify these bases that are important for translocation, the reaction mixture was irradiated with ultraviolet light to form the site-specific cross-link between P site bound 3'-biotin-$tRNA_1^{Val}$ and 16S rRNA (Figure 1D). This cross-link occurred only in ribosomes that have undergone translocation because they contain the 3'-biotin-$tRNA_1^{Val}$ properly positioned in the P site. The samples were extracted using phenol and chloroform and the rRNAs recovered by ethanol precipitation. 16S rRNAs cross-linked to 3'-biotin-$tRNA_1^{Val}$ were captured using magnetic streptavidin beads and the rRNAs were analyzed by primer extension (Figure 1E). Bases that are critical for translocation were identified by comparing the modification levels in the total population versus the selected subpopulation. Bases that are important for translocation lost their functional competence by the modification and therefore are underrepresented in the 16S rRNA from post-translocation ribosomes captured by the cross-link to 3'-biotin-$tRNA_1^{Val}$.

Primer extension analysis revealed a decreased level of modification of nucleotides U56, G529, G530, A532, U723, A1306, A1319, A1408, A1468, A1492, and A1493 in 16S rRNA from the selected subpopulation (Figure 2). Positions G529, G530, A532, A1408, A1492, and A1493 correspond to the class I sites that are protected when tRNA is bound to the ribosomal A site (48). These bases were anticipated to show up in the experiment because the ribosome population is never 100% active in binding tRNAs and these A site residues are modified in ribosomes with a vacant A site. Only ribosomes that had a tRNA bound to the A site translocated. The selected 16S rRNAs, therefore, showed the characteristic A site protection pattern. This result confirms that only ribosomes that contain a tRNA in the A site were competent in translocation. Furthermore, the streptavidin captured 16S rRNA subpopulation showed a substantial enrichment for the C1400 cross-linked product compared to the total population, thereby validating the selection scheme (Figure 2F). In addition to the class I sites, bases U56, U723, A1306, A1319, and A1468 were identified by the modification-interference method (Figure 3A and 3B).

Site-Directed Mutagenesis of 16S rRNA Bases

Bases in 16S rRNA that are protected by A site tRNA have been the subject of mutational analysis by several groups and were not analyzed further. The other five bases (U56, U723, A1306, A1319 and A1468) in 16S rRNA identified in this study have not been analyzed by mutational studies. In order to analyze the role of these 16S rRNA bases in translation, we made transition, transversion and deletion at each position by site-directed mutagenesis. Mutant plasmids were introduced into *E. coli* strain (Δ7rrn) in which all seven copies of the rRNA operons have been deleted from the chromosome (36,37). *E. coli* strain (Δ7rrn) survives by expressing the wild-type rRNA genes from a resident plasmid. After several generations, most of the mutant plasmids were able to replace the resident plasmid indicating that the mutations are not lethal to the cell. However, plasmids with U56Δ, A1319C, or A1319Δ mutations were unable to replace the resident plasmid indicating that these mutations are lethal.

We next analyzed the growth rate of *E. coli* strain (Δ7rrn) having mutant plasmids in liquid cultures under exponential growth conditions. Mutations U56G, A1306C, A1306Δ, A1468U, and A1468Δ reduced the growth rate (Table 1), while other mutations at these positions and at U723 did not affect the growth rate (data not shown). We focused our studies on the mutations that were lethal or affected the growth rate to further understand the role of these 16S rRNA bases in protein synthesis.

Mutations reduced polysome formation and affected subunit association

We examined the polysome profile of *E. coli* strain (Δ7rrn) expressing the mutant 16S rRNAs to identify potential defects in 30S subunit assembly and subunit association. Cell extracts were fractionated on sucrose gradients to monitor the relative amounts of 30S subunits, 50S subunits, 70S ribosomes and polysomes (Figure 4). The peaks corresponding to the polysome fractions were slightly reduced in U56G cells relatively to wild-type cells suggesting minor defects, if any, in 30S subunit assembly or subunit association (Figure 4B). Since U56Δ does not support the growth of *E. coli* strain (Δ7rrn), we cannot directly examine the polysome profile of U56Δ ribosomes. Therefore, U56Δ mutant 30S subunits were purified using an MS2 affinity tag from *E. coli* pop 2136 cells (35). *In vitro* subunit association experiments with purified U56Δ 30S subunits were performed to identify potential defects in 70S ribosome formation. Mutant 30S subunits were incubated with wild-type 50S subunits followed by ultracentrifugation in a sucrose gradient to separate the 30S and 50S subunits, and the 70S ribosome. Wild type 30S subunits readily associated with 50S subunits to form 70S ribosomes (Figure 4G). In contrast, U56Δ 30S subunits failed to associate with the 50S subunits to form 70S ribosomes (Figure 4H).

Cells expressing A1306Δ showed reduced amount of polysomes and the peak corresponding to the 70S ribosome was smaller than the 50S subunit peak indicating that this mutant is unable to efficiently form polysomes (Figure 4C). In addition, the peak corresponding to the 30S subunit was bifurcated suggesting potential defects in 30S subunit assembly. The polysome profile for A1306C was similar to A1306Δ, although the 70S peak was larger in this mutant suggesting that A1306C is not as defective as A1306Δ (Figure 4D).

We analyzed the lethal mutants A1319Δ and A1319C by the *in vitro* subunit association experiments. These studies showed that A1319Δ is defective in subunit association (Figure 4I). In contrast, A1319C was able to associate with the 50S subunits to form 70S ribosomes (Figure 4J). Finally, the polysome profile of A1468Δ and A1468U showed very little polysomes and the 70S peak was significantly reduced compared to wild type strain (Figure 4E and 4F). Additionally, the 30S and 50S subunit peaks were larger than the 70S peak in both the mutants indicating that this base is important for 70S formation.

In order to understand the reason for the severe subunit association defect observed with U56Δ and A1319Δ, we analyzed the ribosomal protein (r-protein) content of the 30S subunits by two-dimensional gel electrophoresis (2D gel). 2D gel analysis showed that U56Δ 30S subunits contain reduced amounts of S2, S5, S10, S11, S12, S18, and S21 (at least 2-fold lower amounts of r-protein than control, Supplementary Figure 2D). In contrast, U56G 30S subunits had normal levels of r-proteins (Supplementary Figure 2B). Both, A1319Δ and A1319C mutants showed reduced amounts of S3, S10, S13, S14, and S18 (Supplementary Figure 2E and 2F). However, proteins S3 and S14 was significantly more reduced in A1319Δ than in A1319C. S3, S13 and S14 are located close to A1319 in the ribosome structure (Figure 3F). The loss of additional r-proteins may be due to secondary effects during subunit assembly. Thus, the absence of some of these r-proteins suggests defects in the assembly of the 30S subunit, which may explain the inability of some of these mutant 30S subunits to associate with the 50S subunit to form 70S ribosomes.

Inhibition of *in vitro* protein synthesis

Even though most of the mutations showed varying degrees of defect in the polysome profiles, they supported the growth of *E. coli* strain (Δ7rrn) suggesting that the mutant ribosomes are functional *in vivo*. We, therefore, tested whether purified mutant ribosomes are functional by examining their ability to synthesize the reporter protein Renilla luciferase using an *in vitro* translation assay. Synthesis of Renilla luciferase was monitored in real-time by the luminescence produced when the substrate coelentrazine is hydrolyzed. The synthesis of luciferase was slightly reduced with U56G ribosomes, which agrees with the modest effects on growth (Supplementary Figure 3A). In contrast, U56Δ ribosomes produced very little luminescence indicating that they are essentially inactive in this assay (Supplementary Figure 3B). This is consistent with the severe subunit association defect observed for U56Δ and the inability to support growth of *E. coli* strain (Δ7rrn). A1306C showed no defects in the *in vitro* translation assay, while A1306Δ showed reduced activity. The activity of A1319C was significantly reduced and A1319Δ was essentially inactive (Supplementary Figure 3B). A1319Δ is defective in subunit association. Interestingly, however, A1319C which did not show a significant subunit association defect showed reduced *in vitro* translation activity. A1319C may potentially be inhibited at a step following subunit association. Finally, although both A1468Δ and A1468U showed reduced level of polysomes, only A1468U showed inhibition in protein synthesis (Supplementary Figure 3A).

Inhibition of tRNA binding

The *in vitro* translation assay showed that ribosomes with the lethal mutations (U56Δ, A1319Δ and A1319C) are not very active in the overall process of protein synthesis. In order to further understand the basis for the inhibition of protein synthesis, we analyzed the mutant ribosomes for defects in tRNA binding using two approaches. First, we used a toeprinting assay to precisely monitor binding of $tRNA^{fMet}$ to the P site (44). Binding of $tRNA^{fMet}$ to the P site produces a reverse transcriptase stop at position +16 of the mRNA, which corresponds to the fraction of mRNA bound to the 30S subunit (Figure 5A). Control experiments showed that in the absence of $tRNA^{fMet}$, no stop is produced at +16 indicating that the mRNA is not stably bound to the 30S subunit under these conditions (Figure 5A, lane 1). Wild-type 30S subunit showed quantitative binding of $tRNA^{fMet}$ to the P site with 1.5-fold excess of $tRNA^{fMet}$ (Figure 5A, lane 2). Similarly U56G ribosomes showed no defects in tRNA binding (≈100% bound) (Figure 5C). In contrast, U56Δ mutant 30S subunits did not bind tRNA even with 10-fold excess $tRNA^{fMet}$ (≈10% bound) (Figure 5A). Slightly reduced $tRNA^{fMet}$ binding was observed with A1306Δ and A1306C (75-80% bound) (Figure 5B). A1319Δ showed strong reduction (< 10% bound), while A1319C showed a smaller reduction in binding $tRNA^{fMet}$ (≈50% bound) (Figure 5A). Finally, A1468Δ and A1468U showed a slight reduction in binding $tRNA^{fMet}$

(≈80% bound) (Figure 5B). The second assay that we used was equilibrium tRNA filter binding and the overall result that we obtained was consistent with the toeprinting assay (Figure 5C).

It is known that the 70S ribosome has a higher affinity for tRNA than the 30S subunit. Furthermore, tRNA can stabilize the association of the subunits. Therefore, we repeated the toeprinting experiments in the presence of the 50S subunit. As expected, wild type ribosomes efficiently bound $tRNA^{fMet}$ at the lowest concentration (Figure 5A, right panel). U56Δ mutant showed a slight improvement in the presence of the 50S subunit, although binding was still significantly reduced (≈20% bound) (Figure 5A, right panel). However, A1319Δ and A1319C did not show any improvements in binding $tRNA^{fMet}$ (Figure 5A, right panel).

We next performed chemical modification experiments to examine the integrity of the ribosome structure near the tRNA binding sites. Primer extension analysis showed that the overall structure of the 16S rRNA near the tRNA binding sites appear to be similar in wild-type and mutant ribosomes (Supplementary Figure 4). Differences in the pattern of chemical reactivity of A1319Δ and A1319C compared to wild-type was observed in the vicinity of G966 (Supplementary Figure 4F).

Translocation of mRNA-tRNA complex

Our studies showed that deletion of U56 or A1319 caused severe defect in subunit association and tRNA binding, resulting essentially in inactive 30S subunits. Therefore, U56Δ and A1319Δ were not analyzed further; instead we focused on mutant ribosomes that showed only minor defects in these functional assays. We examined the ability of mutant ribosomes to translocate the mRNA-tRNA complex. Mutant ribosomes purified from *E. coli* strain (Δ7rrn) were analyzed separately from ribosomes purified using the MS2 affinity tag and compared with the appropriate wild-type ribosomes. EF-G-dependent translocation of the mRNA-tRNA complex was monitored initially by the toeprinting assay (34,44). Translocation of the mRNA-tRNA complex results in the appearance of a toeprint that is three nucleotides shorter compared to the pre-translocation state (Figure 6A and 6B). The extent of translocation was similar by the wild type, U56G, A1306Δ, A1306C, A1319C, A1468Δ and A1468U ribosomes (> 90% translocation). These results show that the mutant ribosomes can form authentic pre-translocation complexes and are able to translocate the mRNA-tRNA complex on adding EF-G.

In order to detect any differences in the rate of translocation, we determined the pre-steady state kinetics of mRNA-tRNA translocation using a fluorescence-based, stopped-flow method (45). Wild-type and mutant ribosomes were used to form pre-translocation complexes and the translocation rate was determined with 5-fold excess EF-G. The time course of translocation showed two phases: a rapid phase ($k_{obs1} \approx 20\ s^{-1}$) followed by a much slower phase ($k_{obs2} \approx 2\ s^{-1}$) (Figure 6C and 6D). The reason for the slow phase is not known and may be due to sample heterogeneity (7). Wild type, A1306C, A1306Δ, A1468U and A1468Δ ribosomes translocated the mRNA-tRNA complex with similar rates (Figure 6C and Table 2). In contrast, the rate of translocation by U56G mutant ribosomes ($k_{obs1} = 12\ s^{-1}$) was ≈2-fold lower than the wild-type ribosomes (Figure 6C and Table 2). In the case of A1319C ribosomes, the rate of fast phase was not affected ($k_{obs1} = 21\ s^{-1}$) (Figure 6D and Table 2). However, the amplitude of the fast phase was reduced by 85% and translocation proceeded mainly by the slow phase ($k_{obs2} = 0.4\ s^{-1}$).

Discussion

Translocation of tRNAs is a complex process involving large-scale structural rearrangements by the ribosome. The rRNAs, which intimately interact with the mRNA and the tRNAs, are likely to play a critical role during translocation. It is often difficult to predict the functional

role of specific bases from the high-resolution crystal structures of the ribosomes. We developed a new modification-interference method to identify bases in 16S rRNA that are important for tRNA translocation. The modification-interference method identified eleven bases of which six bases are located in the A site and are protected when tRNA binds (48). The bases that are protected by A site tRNA are located in the decoding region of the 30S subunit (Figure 4B) (49) and are important for tRNA selection (39) and EF-G-dependent translocation (29).

In addition to the bases protected by A site tRNA, our modification-interference analysis identified five new bases that may play a role in translocation (Figure 3A). The modification-interference assay relied on chemically modifying the base to inhibit translocation. Chemically modifying a base may not have the same effect as mutating a base, especially when bulky groups are added to the base. Nevertheless, we carried out single base substitutions and deletion at each of these positions to investigate their role in protein synthesis. Some of the substitutions had no effect on growth rate; in contrast, U56Δ, A1319C and A1319Δ were unable to support the growth of *E. coli* strain (Δ7rrn) (summarized in Table 3). Insights into the possible role of these five bases in translation are discussed below.

The 30S subunit from U56Δ is missing several r-proteins and is inactive in subunit association. In addition, U56Δ ribosomes are unable to bind tRNA and translate a reporter protein *in vitro*. These results are consistent with the inability of U56Δ to replace the resident wild-type plasmid in *E. coli* strain (Δ7rrn). In contrast, U56G is able to support the growth of *E. coli* strain (Δ7rrn) at a reduced growth rate. U56G appear to be normal in polysome formation, r-protein content, and tRNA binding. Interestingly, U56G showed a 2-fold reduction in the rate of translocation (Figure 6C and Table 2). Nucleotide U56 is universally conserved among all three phylogenetic kingdoms (50) and is located in helix 5 within the body of the 30S subunit (Figure 3B) (51). This region of the 16S rRNA was cleaved by hydroxyl radicals emanating from Fe-EDTA tethered to amino acids 37 and 65 within domain II of EF-G in the fusidic acid stabilized post-translocation complex (52). In addition, positions 55 and 57 in 16S rRNA are protected from hydroxyl radicals in both EF-G•GDPNP complex and fusidic acid stabilized complex (53). These results are in agreement with cryo-EM studies, which showed that domain II of EF-G interacts with helix 5 (14). Modification by CMCT adds the bulky CMC group at the N3 position of U56, which may interfere with EF-G binding or activity.

Position U723 is a bulged nucleotide located in helix 23a within the platform of the 30S subunit (Figure 3B). It is selectively conserved in bacteria and archaea (>90% conserved) (50). Our studies showed that mutation or deletion of U723 does not affect the growth rate, indicating that the base is not essential for translation. However, it is interesting that U723 interacts with the minor groove of the Shine-Dalgarno (SD) helix (Figure 3C) (54, 55). Modification of U723 by CMCT may cause a steric clash with the SD helix and inhibit the movement of the mRNA during translocation. This may explain why modification at U723 is underrepresented in the selected population.

Positions A1306 and A1319 are conserved residues (>98% conservation) located in helix 42 within the head of the 30S subunit (Figure 3B) (51, 56). A1306Δ and A1306C showed reduced growth rate, defects in polysome formation and a slight inhibition in binding tRNA. However, the rate of translocation was not decreased in A1306Δ and A1306C (Table 2). In contrast, deletion of A1319 is lethal and the mutant 30S subunits fail to associate with the 50S subunit. Furthermore, A1319Δ binds tRNA poorly and is inactive in protein synthesis. Similarly, A1319C is also lethal, but the mutant 30S subunit is able to associate with the 50S subunit, bind tRNA with better efficiency and is partially active in proteins synthesis *in vitro*. Interestingly, A1319C showed an 85% decrease in the amplitude of the fast phase of translocation indicating that the extent of translocation was reduced. This decrease maybe

caused by reduced tRNA binding (≈50% reduction in tRNA binding; Figure 5). This interpretation is consistent with toeprinting experiments, which showed reduced levels of pre- and post-translocation complexes compared to the wild type ribosomes (Fig 6B, compare intensities for "Pre" and "Post" bands). cryo-EM studies showed that the largest conformational change during translocation occurs in the 30S head domain, especially in helices 39, 41, and 42 of 16S rRNA (57, 58). Therefore, we speculate that chemical modification of bases A1306 and A1319 in helix 42 of 16S rRNA may inhibit the conformational changes that occur during translocation resulting in the modification being underrepresented in the selected population.

Position A1468 is a universally conserved residue located in helix 44 of 16S rRNA (Figure 3). This helix lies at the subunit interface and makes extensive contacts with the 50S subunit (56,59-61). Our results show that A1468Δ and A1468U have reduced growth rate and defects in polysome formation (Table 3). However, A1468Δ and A1468U appeared normal in tRNA binding and in the rate of translocation. These results suggest that A1468 is important for subunit association *in vivo*. Base A1468 is in an internal loop of helix 44, the opposite strand of this loop (positions 1429-1433) forms part of bridge B6 (57). In addition, bases 1433-1434 form tertiary interactions with bases 319-335 in helix 13 (Figure 3E) (56,60,61). The defect in subunit association may result from the A1468U mutation forming a base pair with one of the nucleotides in the opposite strand of the loop (AGAA), thereby disrupting bridge B6. Alternatively, the A1468U mutation may cause a structural perturbation that misaligns helix 44 relative to the rest of the 30S subunit thereby weakening its association with the 50S subunit. Cryo-EM studies indicate that the small and large ribosomal subunits undergo a ratchet-like rotation (RSR) relative to each other during translocation (57,58). The pivot axis for the RSR is located close to A1468. It is possible that chemical modification of A1468 may interfere with the coordinated movement of the two subunits relative to each other during translocation.

Supplementary Material

Refer to Web version on PubMed Central for supplementary material.

Acknowledgments

We thank Ulrich Muller, Byron Hetrick, and Prashant Khade for helpful comments on the manuscript.

† This work was supported by a grant from the National Institutes of Health, USA (GM65265 to S.J).

Abbreviations

rRNA, ribosomal RNA; EF-G, elongation factor G; GTP, guanosine 5'-triphosphate; DMS, dimethyl sulfate; CMCT, 1-cyclohexyl-3-(2-morpholinoethyl) carbodiimide metho-*p*-toluene sulfonate.

References

1. Moazed D, Noller HF. Intermediate states in the movement of transfer RNA in the ribosome. Nature 1989;342:142–148. [PubMed: 2682263]
2. Odom OW, Picking WD, Hardesty B. Movement of tRNA but not the nascent peptide during peptide bond formation on ribosomes. Biochemistry 1990;29:10734–10744. [PubMed: 1703007]
3. Rodnina MV, Savelsbergh A, Katunin VI, Wintermeyer W. Hydrolysis of GTP by elongation factor G drives tRNA movement on the ribosome. Nature 1997;385:37–41. [PubMed: 8985244]
4. Dorner S, Brunelle JL, Sharma D, Green R. The hybrid state of tRNA binding is an authentic translation elongation intermediate. Nat Struct Mol Biol 2006;13:234–241. [PubMed: 16501572]
5. Pan D, Kirillov SV, Cooperman BS. Kinetically competent intermediates in the translocation step of protein synthesis. Mol Cell 2007;25:519–529. [PubMed: 17317625]

6. Ermolenko DN, Spiegel PC, Majumdar ZK, Hickerson RP, Clegg RM, Noller HF. The antibiotic viomycin traps the ribosome in an intermediate state of translocation. Nat Struct Mol Biol. 2007
7. Walker SE, Shoji S, Pan D, Cooperman BS, Fredrick K. Role of hybrid tRNA-binding states in ribosomal translocation. Proc Natl Acad Sci U S A 2008;105:9192–9197. [PubMed: 18591673]
8. Julian P, Konevega AL, Scheres SH, Lazaro M, Gil D, Wintermeyer W, Rodnina MV, Valle M. Structure of ratcheted ribosomes with tRNAs in hybrid states. Proc Natl Acad Sci U S A 2008;105:16924–16927. [PubMed: 18971332]
9. Agirrezabala X, Lei J, Brunelle JL, Ortiz-Meoz RF, Green R, Frank J. Visualization of the hybrid state of tRNA binding promoted by spontaneous ratcheting of the ribosome. Mol Cell 2008;32:190–197. [PubMed: 18951087]
10. Spiegel PC, Ermolenko DN, Noller HF. Elongation factor G stabilizes the hybrid-state conformation of the 70S ribosome. Rna 2007;13:1473–1482. [PubMed: 17630323]
11. Agrawal RK, Heagle AB, Penczek P, Grassucci RA, Frank J. EF-G-dependent GTP hydrolysis induces translocation accompanied by large conformational changes in the 70S ribosome. Nat Struct Biol 1999;6:643–647. [PubMed: 10404220]
12. Frank J, Agrawal RK. A ratchet-like inter-subunit reorganization of the ribosome during translocation. Nature 2000;406:318–322. [PubMed: 10917535]
13. Stark H, Rodnina MV, Wieden HJ, van Heel M, Wintermeyer W. Large-scale movement of elongation factor G and extensive conformational change of the ribosome during translocation. Cell 2000;100:301–309. [PubMed: 10676812]
14. Connell SR, Takemoto C, Wilson DN, Wang H, Murayama K, Terada T, Shirouzu M, Rost M, Schuler M, Giesebrecht J, Dabrowski M, Mielke T, Fucini P, Yokoyama S, Spahn CM. Structural basis for interaction of the ribosome with the switch regions of GTP-bound elongation factors. Mol Cell 2007;25:751–764. [PubMed: 17349960]
15. Cundliffe, E. The Ribosome. Structure, Function, and Evolution. Hill, WE.; Dahlberg, A.; Garrett, RA.; Moore, PB.; Schlessinger, D.; Warner, JR., editors. Am. Soc. Microbiol.; Washington DC: 1990. p. 479-490.
16. Thompson J, Cundliffe E, Dahlberg AE. Site-directed mutagenesis of Escherichia coli 23 S ribosomal RNA at position 1067 within the GTP hydrolysis centre. J Mol Biol 1988;203:457–465. [PubMed: 2462056]
17. Rosendahl G, Douthwaite S. The antibiotics micrococcin and thiostrepton interact directly with 23S rRNA nucleotides 1067A and 1095A. Nucleic Acids Res 1994;22:357–363. [PubMed: 8127673]
18. Moazed D, Noller HF. Interaction of antibiotics with functional sites in 16S ribosomal RNA. Nature 1987;327:389–394. [PubMed: 2953976]
19. Moazed D, Noller HF. Chloramphenicol, erythromycin, carbomycin and vernamycin B protect overlapping sites in the peptidyl transferase region of 23S ribosomal RNA. Biochimie 1987;69:879–884. [PubMed: 3122849]
20. Carter AP, Clemons WM, Brodersen DE, Morgan-Warren RJ, Wimberly BT, Ramakrishnan V. Functional insights from the structure of the 30S ribosomal subunit and its interactions with antibiotics. Nature 2000;407:340–348. [PubMed: 11014183]
21. Brodersen DE, Clemons WM Jr. Carter AP, Morgan-Warren RJ, Wimberly BT, Ramakrishnan V. The structural basis for the action of the antibiotics tetracycline, pactamycin, and hygromycin B on the 30S ribosomal subunit. Cell 2000;103:1143–1154. [PubMed: 11163189]
22. Harms JM, Wilson DN, Schluenzen F, Connell SR, Stachelhaus T, Zaborowska Z, Spahn CM, Fucini P. Translational regulation via L11: molecular switches on the ribosome turned on and off by thiostrepton and micrococcin. Mol Cell 2008;30:26–38. [PubMed: 18406324]
23. Borovinskaya MA, Shoji S, Holton JM, Fredrick K, Cate JH. A steric block in translation caused by the antibiotic spectinomycin. ACS Chem Biol 2007;2:545–552. [PubMed: 17696316]
24. Moazed D, Robertson JM, Noller HF. Interaction of elongation factors EF-G and EF-Tu with a conserved loop in 23S RNA. Nature 1988;334:362–364. [PubMed: 2455872]
25. Skold SE. Chemical crosslinking of elongation factor G to the 23S RNA in 70S ribosomes from Escherichia coli. Nucleic Acids Res 1983;11:4923–4932. [PubMed: 6348702]
26. Lill R, Robertson JM, Wintermeyer W. Binding of the 3' terminus of tRNA to 23S rRNA in the ribosomal exit site actively promotes translocation. EMBO J 1989;8:3933–3938. [PubMed: 2583120]

27. Feinberg JS, Joseph S. Identification of molecular interactions between P site tRNA and the ribosome essential for translocation. Proc Natl Acad Sci U S A 2001;98:11120–11125. [PubMed: 11562497]
28. Phelps SS, Jerinic O, Joseph S. Universally conserved interactions between the ribosome and the anticodon stem-loop of A site tRNA important for translocation. Mol. Cell 2002;10:799–807. [PubMed: 12419224]
29. Garcia-Ortega L, Stephen J, Joseph S. Precise alignment of peptidyl tRNA by the decoding center is essential for EF-G-dependent translocation. Mol Cell 2008;32:292–299. [PubMed: 18951096]
30. von Ahsen U, Noller HF. Identification of bases in 16S rRNA essential for tRNA binding at the 30S ribosomal P site. Science 1995;267:234–237. [PubMed: 7528943]
31. Yoshizawa S, Fourmy D, Puglisi JD. Recognition of the codon-anticodon helix by ribosomal RNA. Science 1999;285:1722–1725. [PubMed: 10481006]
32. Bocchetta M, Xiong L, Mankin AS. 23S rRNA positions essential for tRNA binding in ribosomal functional sites. Proc Natl Acad Sci U S A 1998;95:3525–3530. [PubMed: 9520399]
33. Stern S, Moazed D, Noller HF. Structural analysis of RNA using chemical and enzymatic probing monitored by primer extension. Methods Enzymol 1988;164:481–489. [PubMed: 2468070]
34. Joseph S, Noller HF. EF-G-catalyzed translocation of anticodon stem-loop analogs of transfer RNA in the ribosome. EMBO J 1998;17:3478–3483. [PubMed: 9628883]
35. Youngman EM, Brunelle JL, Kochaniak AB, Green R. The active site of the ribosome is composed of two layers of conserved nucleotides with distinct roles in peptide bond formation and peptide release. Cell 2004;117:589–599. [PubMed: 15163407]
36. Asai T, Condon C, Voulgaris J, Zaporojets D, Shen B, Al-Omar M, Squires C, Squires CL. Construction and initial characterization of Escherichia coli strains with few or no intact chromosomal rRNA operons. J Bacteriol 1999;181:3803–3809. [PubMed: 10368156]
37. Asai T, Zaporojets D, Squires C, Squires CL. An Escherichia coli strain with all chromosomal rRNA operons inactivated: complete exchange of rRNA genes between bacteria. Proc Natl Acad Sci U S A 1999;96:1971–1976. [PubMed: 10051579]
38. Ron EZ, Kohler RE, Davis BD. Polysomes extracted from Escherichia coli by freeze-thaw-lysozyme lysis. Science 1966;153:1119–1120. [PubMed: 5331371]
39. Cochella L, Brunelle JL, Green R. Mutational analysis reveals two independent molecular requirements during transfer RNA selection on the ribosome. Nat Struct Mol Biol 2007;14:30–36. [PubMed: 17159993]
40. Bartetzko A, Nierhaus KH. Mg2+/NH4+/polyamine system for polyuridine-dependent polyphenylalanine synthesis with near in vivo characteristics. Methods Enzymol 1988;164:650–658. [PubMed: 3071686]
41. Dabrowski M, Spahn CM, Schafer MA, Patzke S, Nierhaus KH. Protection patterns of tRNAs do not change during ribosomal translocation. J Biol Chem 1998;273:32793–32800. [PubMed: 9830024]
42. Nierhaus, K. Ribosomes and Protein Synthesis: A Practical Approach. Spedding, G., editor. IRL Press; Oxford: 1990. p. 161-189.
43. Geyl D, Bock A, Isono K. An improved method for two-dimensional gel-electrophoresis: analysis of mutationally altered ribosomal proteins of Escherichia coli. Mol Gen Genet 1981;181:309–312. [PubMed: 7017346]
44. Hartz D, McPheeters DS, Traut R, Gold L. Extension inhibition analysis of translation initiation complexes. Methods Enzymol 1988;164:419–425. [PubMed: 2468068]
45. Studer SM, Feinberg JS, Joseph S. Rapid Kinetic Analysis of EF-G-dependent mRNA Translocation in the Ribosome. J Mol Biol 2003;327:369–381. [PubMed: 12628244]
46. Schwartz I, Ofengand J. Photochemical cross-linking of unmodified acetylvalyl-tRNA to 16S RNA at the ribosomal P site. Biochemistry 1978;17:2524–2530. [PubMed: 354688]
47. Ofengand J, Liou R, Kohut J. d. Schwartz I, Zimmermann RA. Covalent cross-linking of transfer ribonucleic acid to the ribosomal P site. Mechanism and site of reaction in transfer ribonucleic acid. Biochemistry 1979;18:4322–4332. [PubMed: 385051]
48. Moazed D, Noller HF. Transfer RNA shields specific nucleotides in 16S ribosomal RNA from attack by chemical probes. Cell 1986;47:985–994. [PubMed: 2430725]

49. Ogle JM, Brodersen DE, Clemons WM Jr. Tarry MJ, Carter AP, Ramakrishnan V. Recognition of cognate transfer RNA by the 30S ribosomal subunit. Science 2001;292:897–902. [PubMed: 11340196]
50. Cannone JJ, Subramanian S, Schnare MN, Collett JR, D'Souza LM, Du Y, Feng B, Lin N, Madabusi LV, uuml, ller KM, Pande N, Shang Z, Yu N, Gutell RR. The Comparative RNA Web (CRW) Site: an online database of comparative sequence and structure information for ribosomal, intron, and other RNAs. BMC Bioinformatics 2002;3:2. [PubMed: 11869452]
51. Wimberly BT, Brodersen DE, Clemons WM Jr. Morgan-Warren RJ, Carter AP, Vonrhein C, Hartsch T, Ramakrishnan V. Structure of the 30S ribosomal subunit. Nature 2000;407:327–339. [PubMed: 11014182]
52. Wilson KS, Noller HF. Mapping the position of translational elongation factor EF-G in the ribosome by directed hydroxyl radical probing. Cell 1998;92:131–139. [PubMed: 9489706]
53. Wilson KS, Nechifor R. Interactions of translational factor EF-G with the bacterial ribosome before and after mRNA translocation. J Mol Biol 2004;337:15–30. [PubMed: 15001349]
54. Korostelev A, Trakhanov S, Asahara H, Laurberg M, Lancaster L, Noller HF. Interactions and dynamics of the Shine Dalgarno helix in the 70S ribosome. Proc Natl Acad Sci U S A 2007;104:16840–16843. [PubMed: 17940016]
55. Kaminishi T, Wilson DN, Takemoto C, Harms JM, Kawazoe M, Schluenzen F, Hanawa-Suetsugu K, Shirouzu M, Fucini P, Yokoyama S. A snapshot of the 30S ribosomal subunit capturing mRNA via the Shine-Dalgarno interaction. Structure 2007;15:289–297. [PubMed: 17355865]
56. Schuwirth BS, Borovinskaya MA, Hau CW, Zhang W, Vila-Sanjurjo A, Holton JM, Cate JH. Structures of the bacterial ribosome at 3.5 A resolution. Science 2005;310:827–834. [PubMed: 16272117]
57. Gao H, Sengupta J, Valle M, Korostelev A, Eswar N, Stagg SM, Van Roey P, Agrawal RK, Harvey SC, Sali A, Chapman MS, Frank J. Study of the structural dynamics of the E coli 70S ribosome using real-space refinement. Cell 2003;113:789–801. [PubMed: 12809609]
58. Valle M, Zavialov A, Sengupta J, Rawat U, Ehrenberg M, Frank J. Locking and unlocking of ribosomal motions. Cell 2003;114:123–134. [PubMed: 12859903]
59. Yusupov MM, Yusupova GZ, Baucom A, Lieberman K, Earnest TN, Cate JHD, Noller HF. Crystal Structure of the Ribosome at 5.5 A Resolution. Science 2001;292:883–896. [PubMed: 11283358]
60. Korostelev A, Trakhanov S, Laurberg M, Noller HF. Crystal structure of a 70S ribosome-tRNA complex reveals functional interactions and rearrangements. Cell 2006;126:1065–1077. [PubMed: 16962654]
61. Selmer M, Dunham CM, Murphy F. V. t. Weixlbaumer A, Petry S, Kelley AC, Weir JR, Ramakrishnan V. Structure of the 70S ribosome complexed with mRNA and tRNA. Science 2006;313:1935–1942. [PubMed: 16959973]

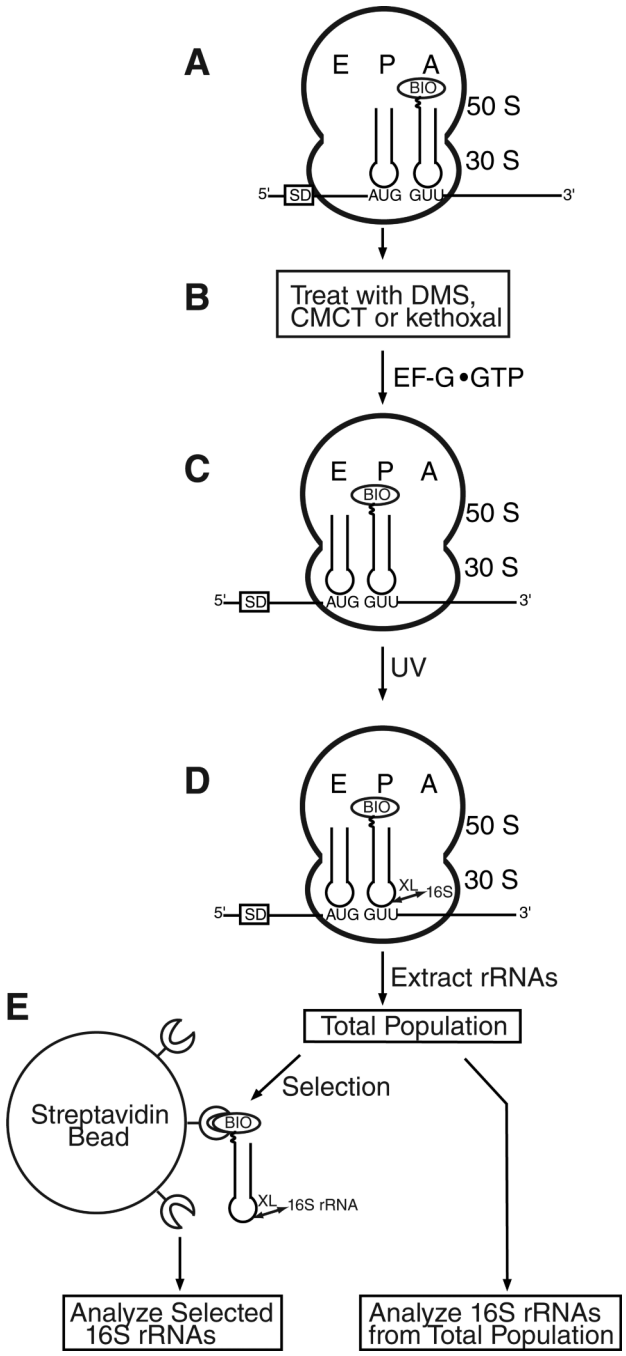

Figure 1. Schematic illustration of the modification-interference method

(A) Pre-translocation complex programmed with gene32val2 mRNA and having $tRNA_f^{Met}$ and 3'-biotin-$tRNA_1^{Val}$ in the P and A sites, respectively. (B) Chemical modification of the complex using DMS, CMCT, or kethoxal. (C) Translocation, catalyzed by EF-G•GTP, results in the movement of 3'-biotin-$tRNA_1^{Val}$ from the ribosomal A site to the P site. (D) Ultraviolet light induces a cross-link between 3'-biotin-$tRNA_1^{Val}$ and 16S rRNA only in the post-translocation complexes. (E) The rRNAs are extracted from the ribosomes and the 16S rRNAs cross-linked to 3'-biotin-$tRNA_1^{Val}$ are captured using magnetic streptavidin beads. The 16S rRNAs from the total population and the selected subpopulation are analyzed in parallel by

primer extension. Abbreviations: BIO, biotinyl group; XL, cross-link, SD, Shine-Dalgarno sequence.

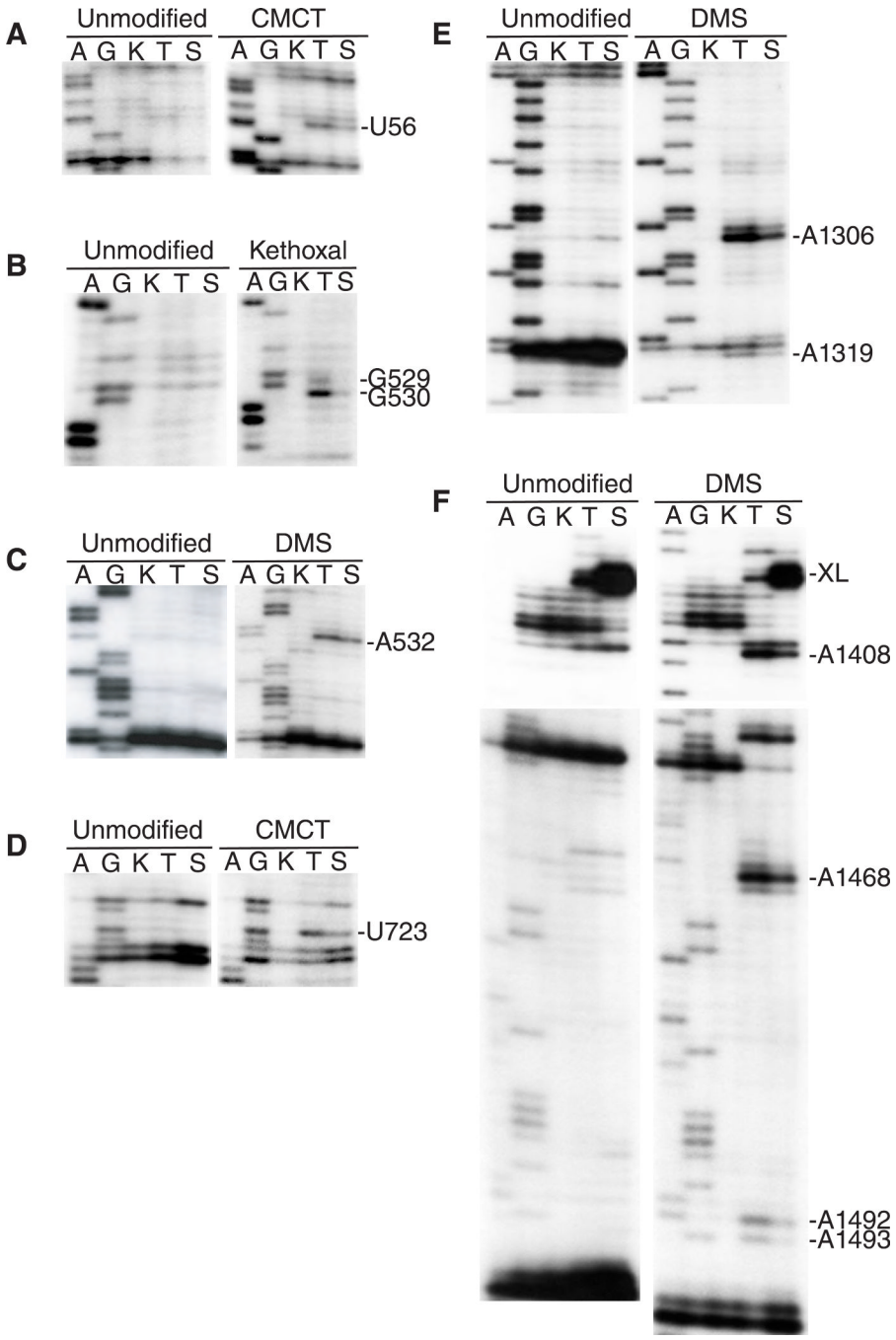

Figure 2. Base modifications of 16S rRNA that interfere with EF-G-dependent translocation

RNA was extracted from the ribosome and the level of modification analyzed by primer extension. rRNA from unmodified ribosomes was analyzed in parallel with either CMCT, kethoxal or DMS treated ribosomes. A and G, dideoxy sequencing lanes; K, unmodified 16S rRNA; T, 16S rRNA from the total population; S, 16S rRNA from the streptavidin-captured subpopulation. The autoradiographs show regions of 16S rRNA around position (A) 56 (CMCT); (B) 530 (kethoxal); (C) 532 (DMS); (D) 723 (CMCT); (E) 1306-1319 (DMS); and (F) 1400-1493 (DMS).

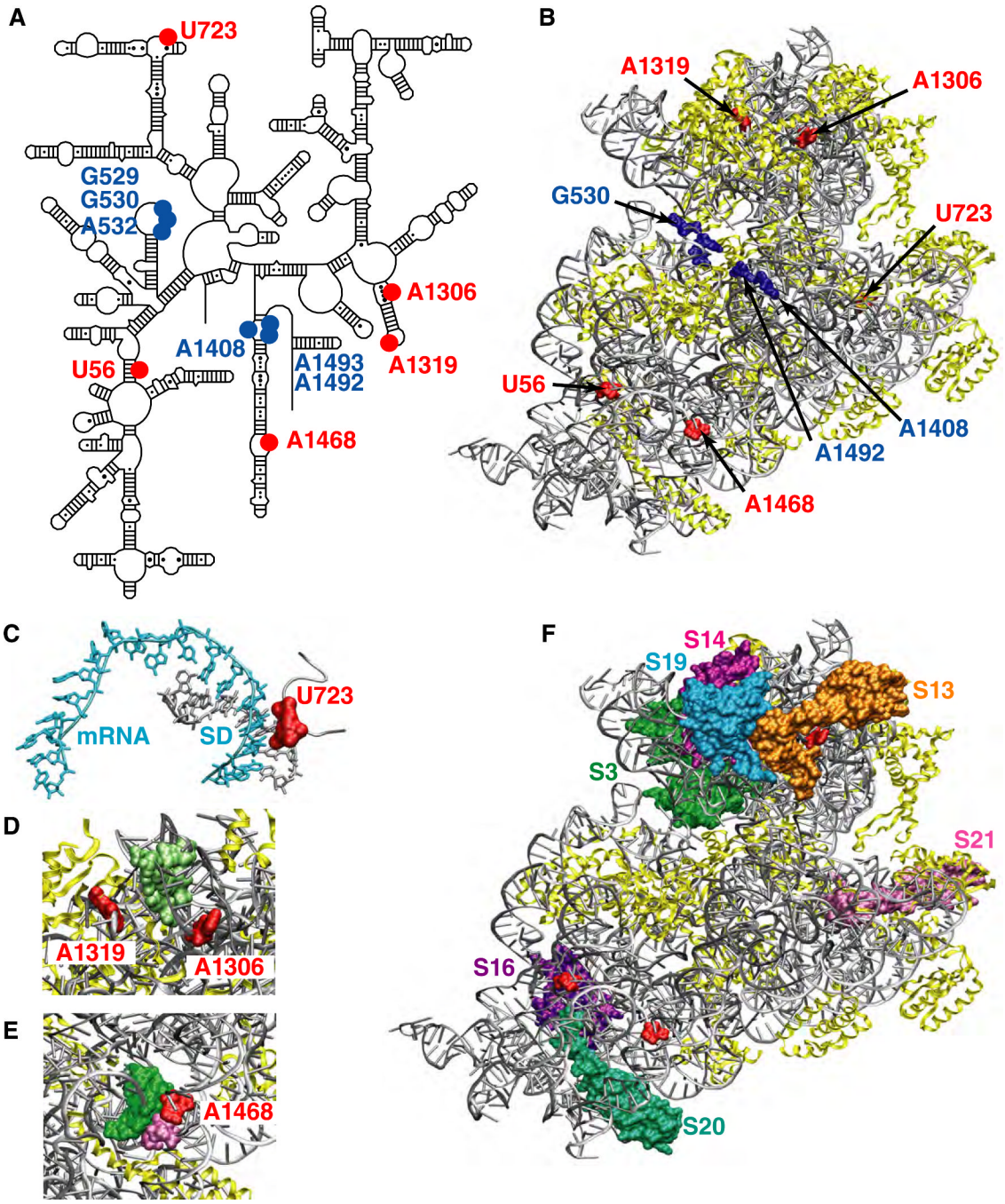

Figure 3. Location of the nucleotides identified by the modification-interference method

(A) Bases that are protected by A site tRNA (blue) and bases newly identified (red) are indicated on the secondary structure of 16S rRNA. (B) Three-dimensional location of nucleotides in the x-ray crystal structure of the *E. coli* 30S subunit (PDB ID code 2AVY). The 16S rRNA and the r-proteins are shown in silver and yellow, respectively. (C) Base U723 interacts with the minor groove of the Shine-Dalgarno helix (PDB ID code 2QNH). mRNA is in cyan and 16S rRNA (1539-1541) is in silver. (D) Tertiary interactions between helix 41 (A1268 and G1269) and helix 42 (base pairs A1311-U1326 and G1312-C1325) are indicated in green. (E) Tertiary interactions between helix 13 (U317 to A336; green) and helix 44 (A1433 and A1434; mauve). (F) Ribosomal proteins in the vicinity of the selected bases. Proteins S16 (violet) and S20

(green) are located close to U56 in the ‘body’ of the 30S subunit. Proteins S3 (dark green), S13 (orange), S14 (magenta) and S19 (cyan) are located close to A1306 and A1319 in the ‘head’ of the 30S subunit. Protein S21 (mauve) is located close to U723 in the ‘platform’ of the 30S subunit. The figures were created using VMD and rendered using POV-Ray.

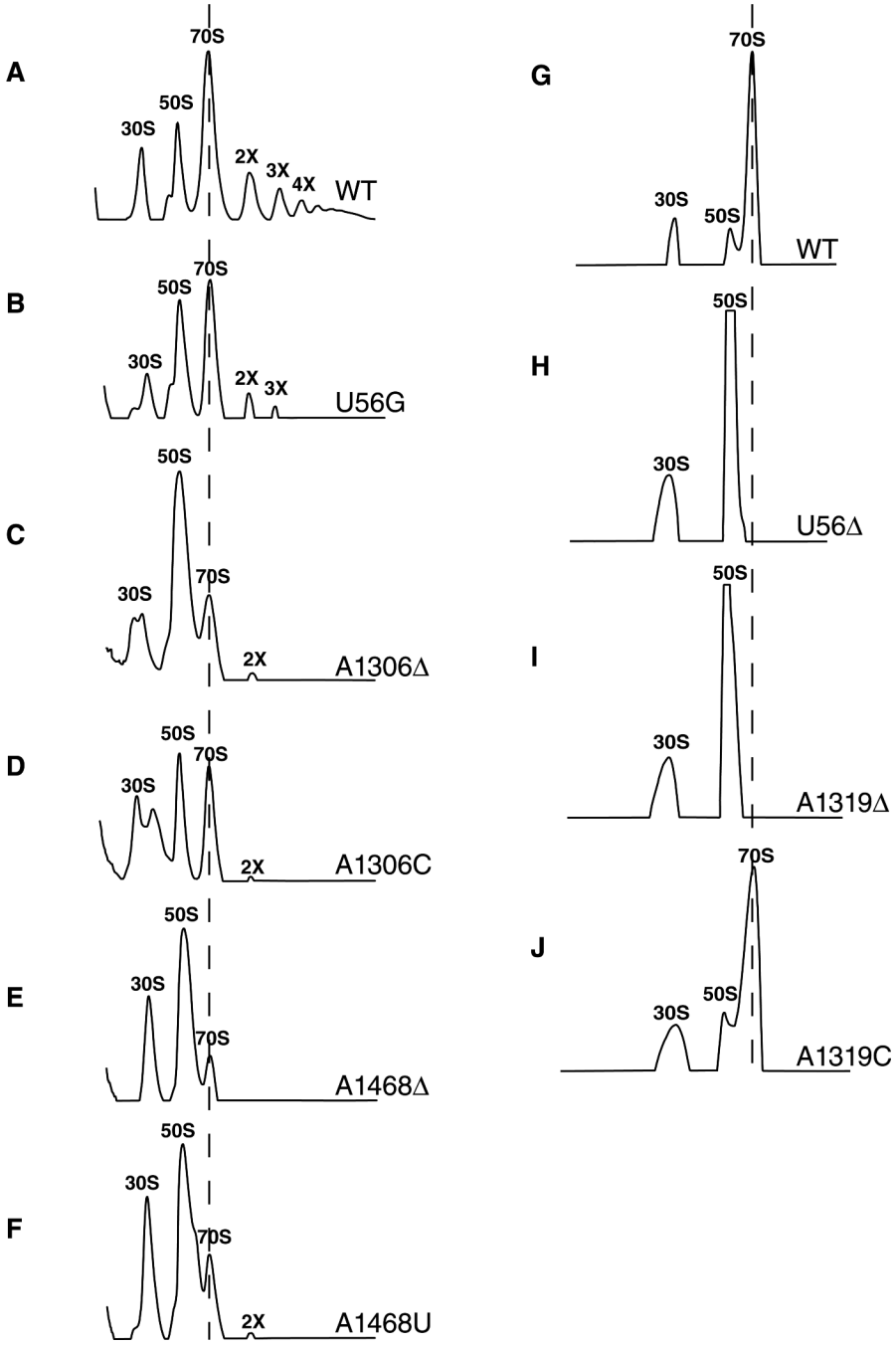

Figure 4. Polysome profile of cells expressing mutant 16S rRNA and subunit association

Polysome profile of cells expressing mutant 16S rRNA in *E. coli* (Δ7rrn) strain. (A) Wild-type control, (B) U56G, (C) A1306Δ, (D) A1306C, (E) A1468Δ, and (F) A1468U mutant 16S rRNA. Labels: 30S, small ribosomal subunits; 50S, large ribosomal subunits; 70S, ribosomes; 2X to 4X, polysomes. The dotted line indicates the position of the 70S ribosome in the gradients. In the case of lethal mutations, association of 30S subunits with the 50S subunits to form 70S ribosomes was analyzed by sucrose gradient centrifugation. (G) Wild-type control, (H) U56Δ, (I) A1319Δ, and (J) A1319C mutant 30S subunits. The experiment was performed in buffer containing 20 mM $MgCl_2$. Labels are as described above.

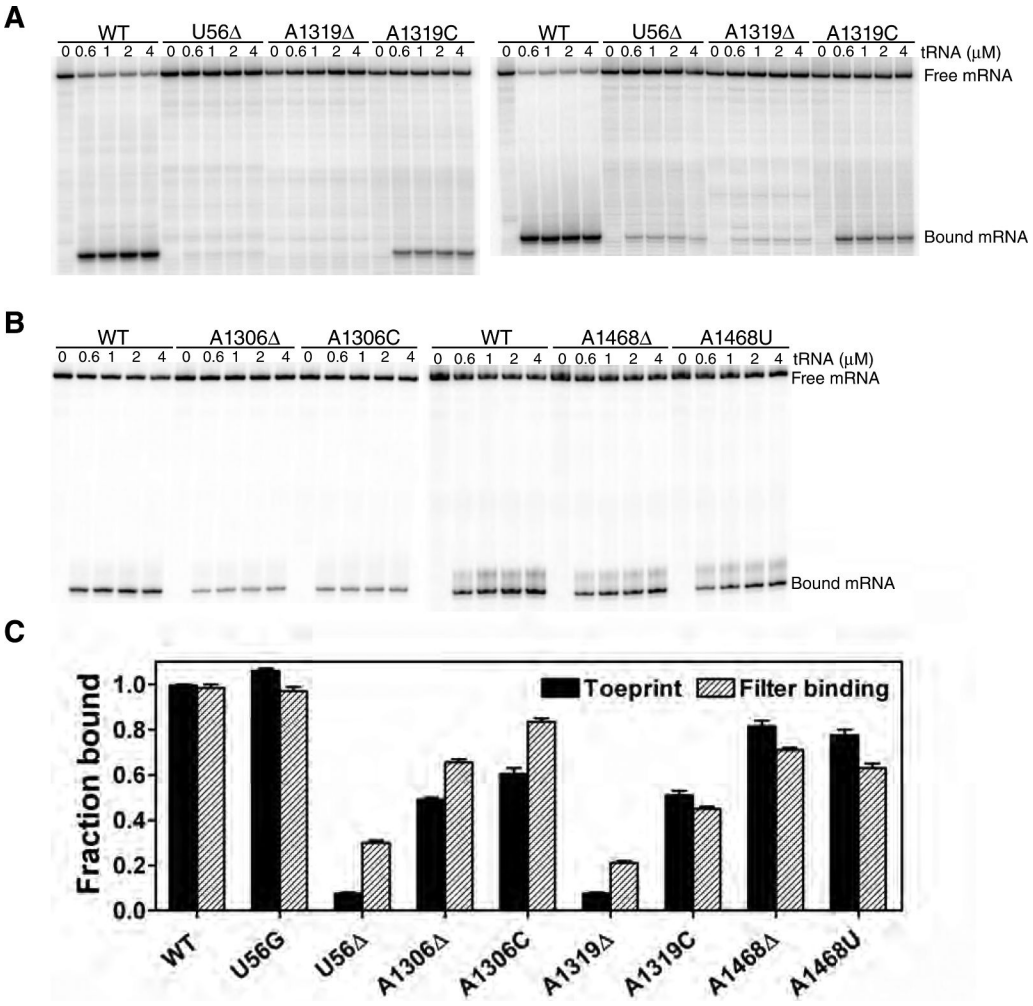

Figure 5. Binding of tRNA to the mutant 30S subunits

Toeprinting assay to monitor binding of $tRNA^{fMet}$ to the ribosomal P site. (A) Binding of tRNA to the 30S subunit (left panel) and to the 70S ribosome (right panel) are shown for mutations that cause a lethal phenotype. The final conc. of tRNAs in the reaction are indicated above the lanes. The toeprints corresponding to the full-length cDNA (free mRNA) and mRNA bound to the 30S subunit are indicated. (B) Binding of tRNA to mutant 30S subunits purified from *E. coli* (Δ7rrn). Labels are as described above. (C) Graph showing the fraction of $tRNA^{fMet}$ bound to the 30S subunit P site. The toeprinting data are indicated by the black bars and the filter binding data are indicated by the striped bars. The standard deviations from at least two experiments are shown.

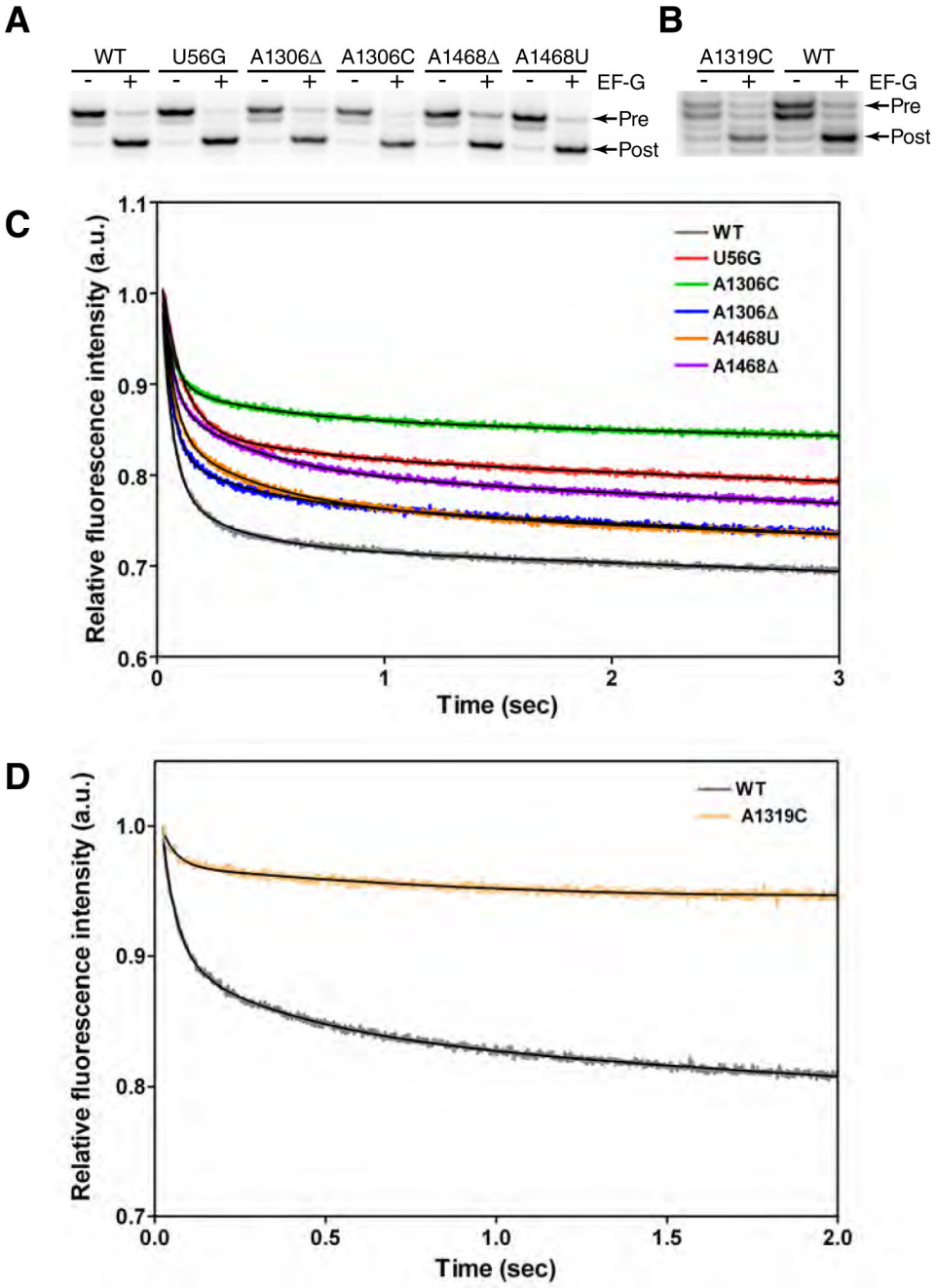

Figure 6. Translocation of mRNA-tRNA complex

(A) The extent of translocation by the mutant ribosomes was determined using the toeprinting assay. '-' and '+' indicate the absence and presence of EF-G, respectively. Toeprints corresponding to the pre-translocation (Pre) and the post-translocation (Post) complexes are indicated. (B) Translocation by affinity purified wild-type and A1319C ribosomes. (C) Pre-steady state kinetic analysis of EF-G-dependent translocation of wild-type and mutant ribosomes. (D) Translocation kinetics of affinity purified wild-type and A1319C ribosomes. The decrease in fluorescence intensity corresponds to EF-G-dependent mRNA-tRNA translocation and was fit to a double exponential equation (black line).

Table 1

Growth rates of *E. coli* expressing mutant 16S rRNAs

Ribosome	Doubling time (min)
WT[a]	41 ± 1
U56G[a]	68 ± 4
A1306Δ[a]	80 ±2
A1306C[a]	81 ± 4
A1468Δ[a]	60 ± 1
WT[b]	61 ± 3
A1468U[b]	100 ± 5

The mean ± standard deviations of ten growth curves are indicated.

[a] plasmid pLK35 was used to express rRNAs.

[b] plasmid pKK3535 was used to express rRNAs.

Table 2

Pre-steady state rate of translocation by mutant ribosomes

Ribosome	k_{obs1} (s^{-1})	A_1	k_{obs2} (s^{-1})	A_2
WT	18.4 ± 0.7	0.32 ± 0.01	2.9 ± 0.4	0.06 ± 0.005
U56G	11.9 ± 0.8	0.21 ± 0.01	2.1 ± 0.5	0.04 ± 0.007
A1306Δ	23.5 ± 0.8	0.33 ± 0.01	2.8 ± 0.3	0.06 ± 0.003
A1306C	20.9 ± 2.7	0.16 ± 0.02	2.3 ± 0.2	0.04 ± 0.005
A1468Δ	24.3 ± 0.7	0.25 ± 0.01	2.5 ± 0.1	0.09 ± 0.002
A1468U	22.0 ± 1.4	0.29 ± 0.02	2.4 ± 0.1	0.09 ± 0.003
WT (MS2)	21.3 ± 2.0	0.16 ± 0.01	2.4 ± 0.2	0.07 ± 0.003
A1319C (MS2)	20.9 ± 2.4	0.04 ± 0.01	0.4 ± 0.1	0.15 ± 0.02

The mean ± standard deviations of four experiments are shown. MS2, indicates ribosomes purified using the MS2 affinity tag.

Table 3

Summary of defects caused by mutations in 16S rRNA

Activity	U56Δ	U56G	A1306Δ	A1306C	A1319Δ	A1319C	A1468Δ	A1468U
Growth phenotype	Lethal	+++	++	++	Lethal	Lethal	+++	+
Polysome profile	ND	+++	++	++	ND	ND	+	+
Subunit association	-	ND	ND	ND	-	++++	ND	ND
In vitro translation	-	+++	+++	++++	-	+	++++	++
tRNA binding (P-site)	-	++++	+++	+++	-	+++	+++	+++
Translocation rate	ND	++	++++	++++	ND	++++[a]	++++	++++

Lethal, does not support growth of *E. coli* strain (Δ7rrn). (++++) no defect; (+++, ++, +) slight to severe defect, where +++ is slight defect; (-) no detectable activity.

ND, not determined.

[a] the extent of rapid translocation was reduced.